

RESEARCH ARTICLE

## Synthesis of TiO<sub>2</sub> nanorods with a microwave assisted solvothermal method and their application as dye-sensitized solar cells

Hossein Rezvani Nikabadi<sup>1</sup>, Saeed Khosroabadi<sup>2</sup>

<sup>1</sup>Department of Basic Sciences, Imam Reza International University, Mashhad, Iran

<sup>2</sup>Department of Electrical Engineering, Imam Reza International University, Mashhad, Iran

### ARTICLE INFO

#### Article History:

Received 21 Nov 2019

Accepted 29 Jan 2020

Published 1 Feb 2020

#### Keywords:

TiO<sub>2</sub> nanorods

Dye sensitized solar cells

Solvothermal

J-V plot

### ABSTRACT

In this work, Titanium dioxide (TiO<sub>2</sub>) nanostructures have been synthesized via a microwave assisted solvothermal method using titanium tetraisopropoxide (TTIP), polyvinylpyrrolidone (PVP) and Ascorbic Acid (AA) in ethanol. The mole ratio of PVP/AA was found to be critical in determining the morphology and crystal phase of the final product. PVP/AA mole ratio varied from 1 up to 15 to obtain different morphologies of TiO<sub>2</sub>. The structural analysis by XRD diffraction confirmed formation of titanium dioxide. The Williamson-Hall (W-H) analysis was used to study the individual contributions of crystallite sizes and lattice strain on the peak broadening of the TiO<sub>2</sub> nanoparticles. FTIR spectrum was used to estimate the various functional groups present in the nanostructures. Scanning electron microscope (SEM) images demonstrate nanoparticle, short nanorod, and long nanorods for 5, 10 and 15 mole ratio of PVP/AA respectively. TiO<sub>2</sub> nanoparticles and nanorods have been used as photoelectrode in dye-sensitized solar cell (DSSCs) fabrication. The efficiencies of solar cells were calculated 3.23% and 4.01% for nanoparticles and nanorods, respectively.

### How to cite this article

Rezvani Nikabadi H., Khosroabadi S. Synthesis of TiO<sub>2</sub> nanorods with a microwave assisted solvothermal method and their application as dye-sensitized solar cells. J. Nanoanalysis., 2020; 7(1): 21-30. DOI: 10.22034/jna.2019.1877392.1157.

## INTRODUCTION

Air pollution is one of the most important issues, which scientists face with it. Hence, many works have been done to reduce this problem in our surrounding environment. Using renewable energy such as solar energy instead of fossil fuel is one solution for the mentioned problem and photovoltaic cell (PV) [1-3] is a new technology that has attracted enormous interest recently because of inexhaustible, safe and environmentally friendly [4]. It is possible to find different categories of photovoltaic cells in the literature as silicon, copper indium selenite, CdTe, perovskite solar cell [5,6] and dye-sensitized solar cells [7-20].

Among the mentioned photovoltaic cells, Dye-sensitized solar cells (DSSCs) due to the high efficiency and low fabrication cost are more famous than that of the other ones. Moreover,

\* Corresponding Author Email: [rezvaninikabadi@gmail.com](mailto:rezvaninikabadi@gmail.com)

two major requirements in DSSC technology are charge transport through a semiconductor and the electrolyte [4] which it can be possible to increase the electron transport and light trapping by using titanium dioxide (TiO<sub>2</sub>) nanoparticle in DSSCs [21]. TiO<sub>2</sub> is used as an electron transport layer in PV and photoelectrochemical devices and it has been implemented as a photocatalyst [22] and electrode solar cell based on dye-sensitized photo-electrochemical [23-29]. The Various kinds of TiO<sub>2</sub> structures like TiO<sub>2</sub> nanotubes [30] and one-dimensional TiO<sub>2</sub> [31-33] have been used to improve the efficiency of DSSCs.

From the fabrication point of view, different methods were used to fabricate TiO<sub>2</sub> nanostructures, which include these methods: Sol-Gel [34, 35], Micelle and Inverse Micelle, Hydrothermal, Solvothermal [36], Chemical Vapor Deposition, Electrodeposition, Sonochemical and

Table 1. samples with different PVP to AA molar ratios

Sample name	(X= [PVP]/[AA])
S1	1
S2	5
S3	10
S4	15

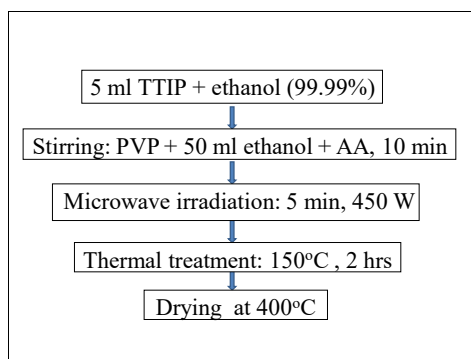


Fig.1. Flowchart of synthesise process.

Microwave [37-39]. Although, the Solvothermal method is more effective because, in this method, low temperature is used to format high particle crystal with high purity Using microwave helped solvothermal technique for quick heating and rapid crystallization rate [40, 41].

Titania nanotubes have been used vastly as a starting material compared to titanium dioxide since they have many hydroxyl groups and capability for ion absorption [42, 43]. Furthermore, it is possible to improve the electron transport as well as light trapping in DSSCs using TiO<sub>2</sub> nanowires and nanorods as scattering layer [44].

In this research, microwave assisted solvothermal method is used to prepare TiO<sub>2</sub> nanorods. We introduce PVP as an effective capping agent for nanorods formation and ascorbic acid as a mild reducing agent in this report for the first time. TiO<sub>2</sub> nanoparticles and nanorods are used as photoelectrode in dye-synthesized solar cell (DSSCs) fabrication.

## EXPERIMENTAL METHOD

### Preparing TiO<sub>2</sub> nanostructures

A mixture of Ti-containing precursor solution based on titanium tetraisopropoxide (TTIP) and polyvinylpyrrolidone (PVP) and Ascorbic Acid (AA) was prepared in 100 ml of ethanol with different molar ratio of TTIP/PVP/AA 1:1:X (X: 1, 5, 10, 15) as mentioned in Table 1. Fig.1 shows

Flowchart of synthesise process. For this solution, 5ml of TTIP was diluted in absolute (99.99%) ethanol. Thereafter, PVP was dissolved in 50 ml of ethanol and added to the first solution. Appropriate volume of AA was also dissolved in this solution and stirred for 10 min. Then the solution was exposed to microwave irradiation for 5 min at 450 W. The microwave treated solution transferred to a Teflon sealed autoclave for solvothermal synthesis and treated at 150°C for 2 h. The obtained powder was washed and calcined at 400°C to remove residual compounds and cooled naturally to room temperature for further analysis and cell fabrication.

### Characterization tools

The crystalline structure of the powders was recorded by D8-Advanced Bruker X-ray diffractometer using Cu-K $\alpha$  radiation ( $\lambda = 1.54056 \text{ \AA}$ ) in the range  $2\theta = 20 - 90$  degrees. SEM images were obtained using LEO 1450VP system. FTIR data were collected using an AVATAR-370-FTIR THERMONICOLET spectrometer using two separate procedures. The sample was unpacked into a tablet shape and put onto a polished silicon wafer before analysis.

### Fabrication and characterization of DSSC

The TiO<sub>2</sub> nanostructure was made by mixing with ethyl cellulose,  $\alpha$ -terpineol and ethanol. The

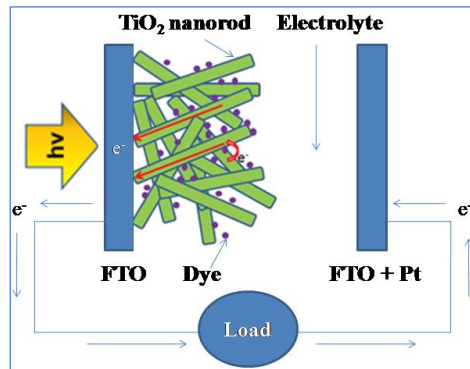


Fig.2. Schematic diagram of the cell structure.

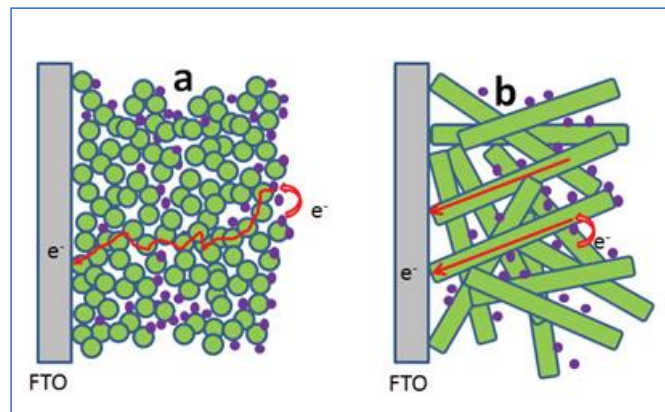


Fig.3. Schematic illustration of electron transportation in the working electrode made of (a) nanoparticles, (b) nanorods.

solution was stirred for 30 minutes. The solution sonicated together with heat treatment at 80°C until became to a viscous paste. A few drops of acetic acid and triton-x-100 added to the solution. The paste was spread on the FTO substrate by applying doctor blade technique. This is known as photoanode. The as prepared photoanode dried at 500°C for calcinations and sintering and finally the electrode was treated in the solution of 40 mM TiCl<sub>4</sub> for 30 min. Next, the photoanode was soaked in 0.3 mM MN719 dye for 24h. After that, the cells were filled with I<sup>-</sup>/I<sup>-3</sup> electrolyte. The counter electrode was Pt fabricated using thermal treatment of H<sub>2</sub>PtCl<sub>4</sub> 5mM at 400°C for 30 min. Figs. 2 and 3 show the schematic diagram of the cell structure.

Two main factors directly affect the photovoltaic properties of a working electrode: surface area of the TiO<sub>2</sub> layer and TiO<sub>2</sub> crystal characteristic. The higher surface area would allow more dye molecules to be absorbed on working electrode,

hence generating more photoelectrons under the same level of excitation, while crystal property is important to electron transport. Electron transport within single crystals is faster than in a particle aggregate because the grain boundaries in the former are much less. In our case, the TiO<sub>2</sub> nanoparticle layer had a very high surface area and dye loading. A large amount of photoelectrons were generated and injected into the nanoparticles. However, the large number of grain boundaries at the nanoparticle interfaces had caused a zigzag pathway of electron transport with ohmic loss. Charge recombination became a major obstacle in efficient energy conversion (Fig. 3a). The nanorods have higher surface area than the nanofibres but lower than the nanoparticles. However, as nanorods were in single-crystalline form, they could provide a better electron pathway for electron transport than nanoparticles (Fig. 3b).

The J-V characteristic of the cells having the

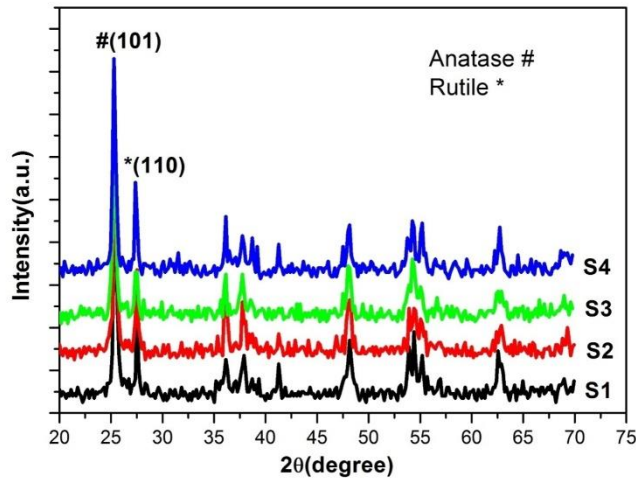


Fig.4. XRD pattern of the samples with different PVP/AA mole ratios.

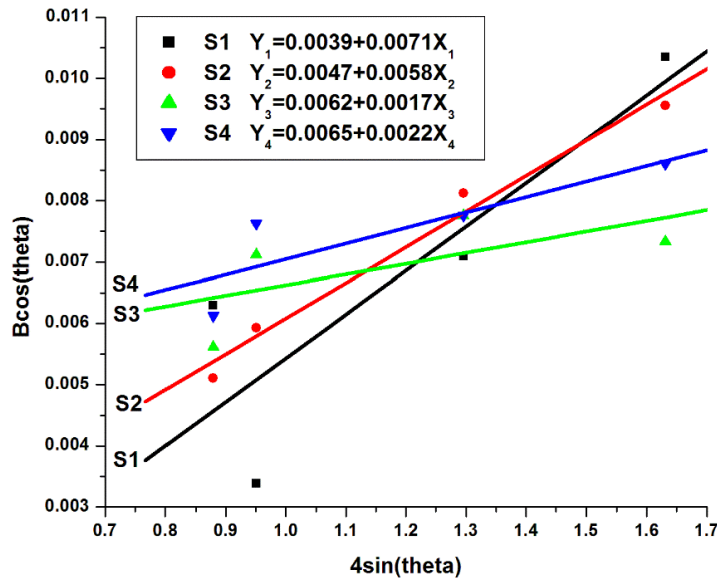


Fig.5. Williamson-Hall plot of samples for determination of lattice strains and mean particle sizes.

active area of 0.16 cm<sup>2</sup> was measured under AM 1.5 (100mWcm<sup>-2</sup>) illuminations using a solar simulator coupled with a Palm SensPotentiostat for recording J-V plots. Incident photon-to-current efficiency (IPCE) was measured using a 150W halogen lamp in combination with a grating monochromator and calibrated by a silicon photodiode.

## RESULTS AND DISCUSSION

Fig.4 shows that the prepared Titanium oxide nanostructures are well crystallized and composed of Anatase and Rutile phase structures.

The (101)-plane for Anatase and (110)-plane for Rutile are the main diffraction planes seen in the figure. The net intensity for (101) shows that the samples are well crystallized. Increase of PVP/AA causes a considerable increase of the net intensity of the main peak of Anatase phase. This is the indication of preferential growth of Anatase phase due to the increase of PVP as capping agent. The mean crystalline size of nanoparticles is estimated using Williamson-Hall method [45, 46] and the results are plotted as Fig.5 and the calculated mean particle size and lattice strain are summed up in

Table 2. Williamson-Hall data of the samples

Sample name	$0.9\lambda/d$	Mean particle size	$\epsilon$ (%) (Lattice strain)
S1	0.0039	35.53	0.71
S2	0.0047	29.48	0.58
S3	0.0062	22.35	0.17
S4	0.0065	21.32	0.22

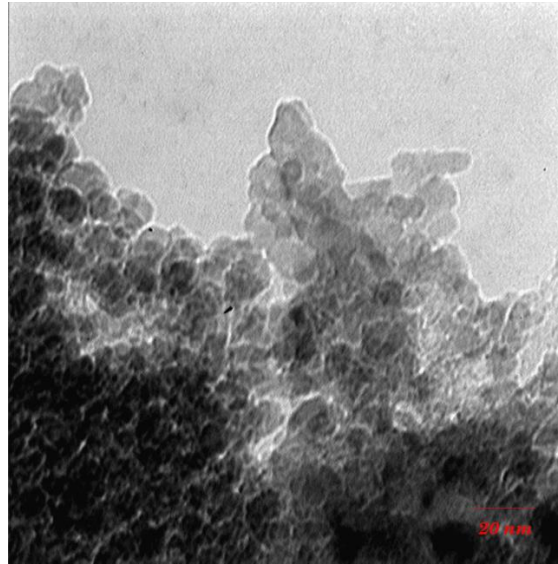


Fig.6. TEM image of TiO<sub>2</sub> nanoparticles.

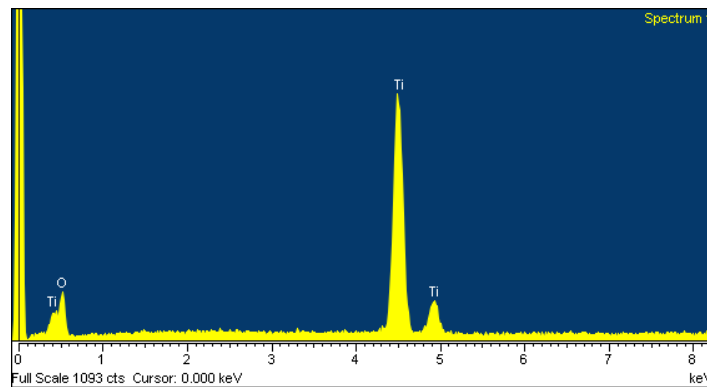


Fig.7. EDX spectrum image of TiO<sub>2</sub> nanoparticles.

Table 2. The mean particle size decreases from S1 to S4as well as the lattice strain accordingly. It is mostly stated that with the decrease of size, lattice strain increases unless the morphology of the particles changes dramatically [47, 48]. It can be stated that the increase of PVP/AA led to change of morphology of the samples.

Fig.6 shows TEM image of TiO<sub>2</sub> nanoparticles

with a narrow size of about 20 nm which was in perfect agreement with the XRD analysis results. The Energy Dispersive X-ray Spectroscopy (EDS) confirms the chemical composition of the prepared TiO<sub>2</sub> nanoparticles (Fig.7).

Fig.8 indicates the FTIR spectra of the samples. There are absorption peaks for the wavenumbers of 2500-4000 cm<sup>-1</sup>that is confirming the presence

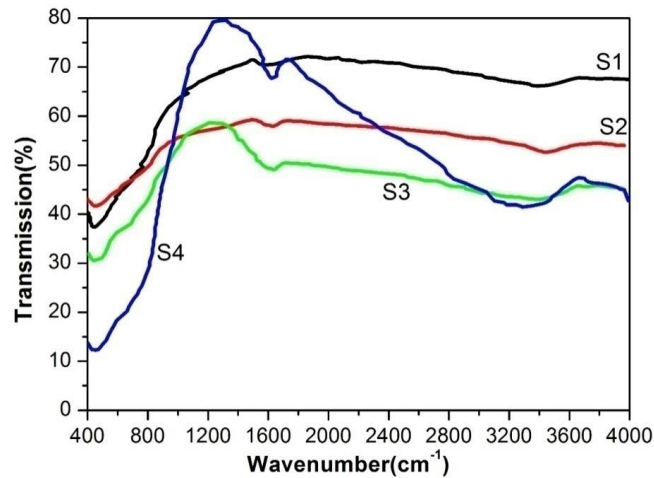


Fig.8. FTIR spectra of the samples.

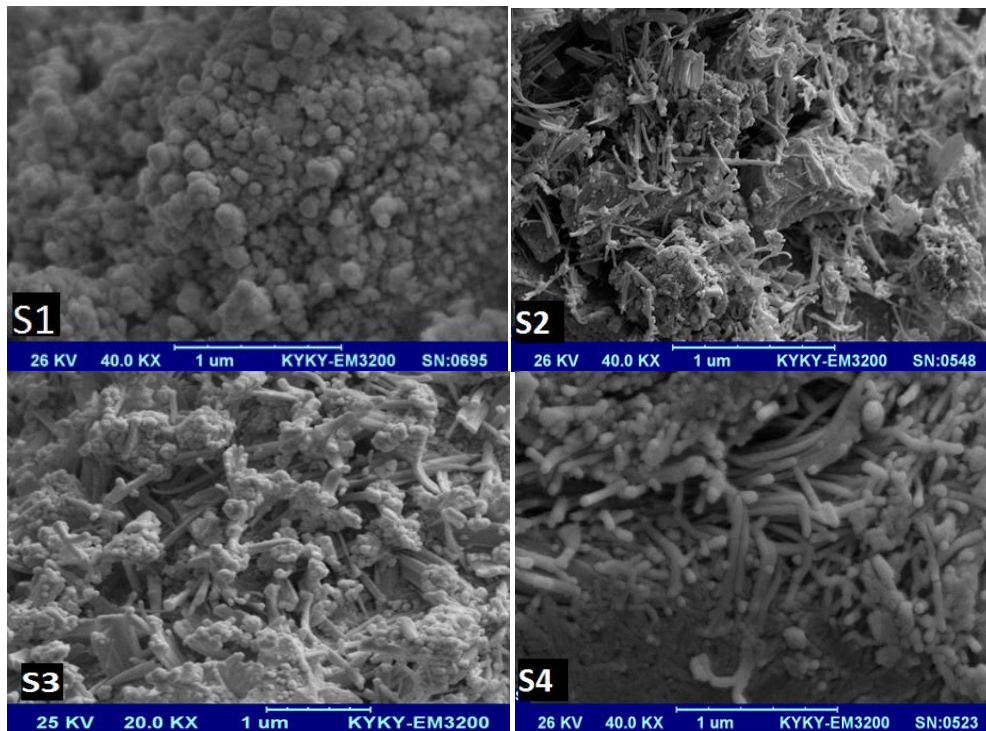


Fig.9. SEM images of the samples.

of compounds of carbon and water. The peaks at  $1640\text{ cm}^{-1}$  in the spectra are due to the stretching and bending vibration of the -OH group. The peak at  $440\text{ cm}^{-1}$  is attributed to Ti-O bond for S1, which shifts to  $442$ ,  $450$  and  $454\text{ cm}^{-1}$  for S2, S3 and S4, respectively. The shift to higher frequencies indicates the shortening of Ti-O bond and simultaneously confirms the reduction of atomic plane distances.

Fig.9 shows SEM images for the samples. Generally, they have uniform size distribution which is the advantage of this method. Nanoparticles transform to nanowire like-structure when PVP/AA mole ratio increased up to 5 (Fig.9-S2). All nanowires are roughly uniform in shape and morphology in large area scale. Fig.9-S3 showed a uniformly long and narrow rod structure with several micrometers length

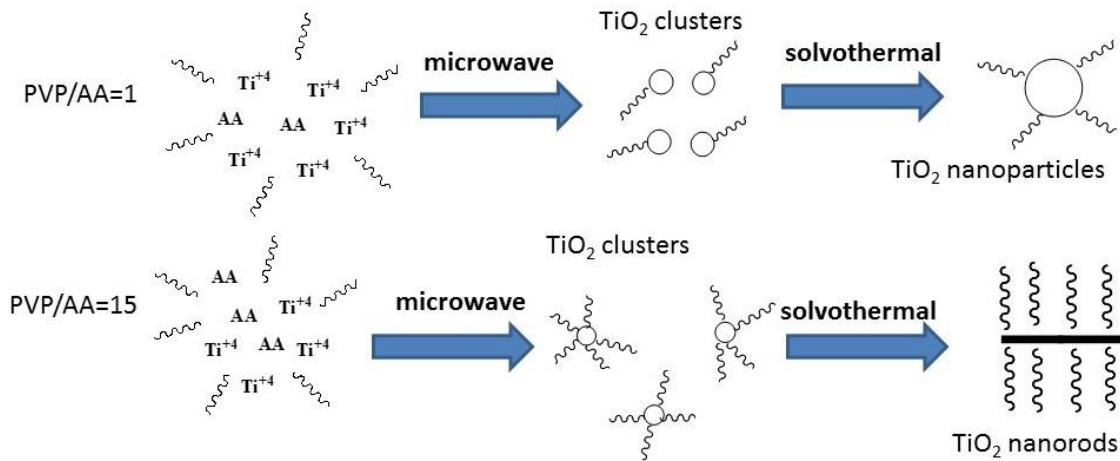


Fig.10. Schematic mechanism of the formation of TiO<sub>2</sub> nanorods.

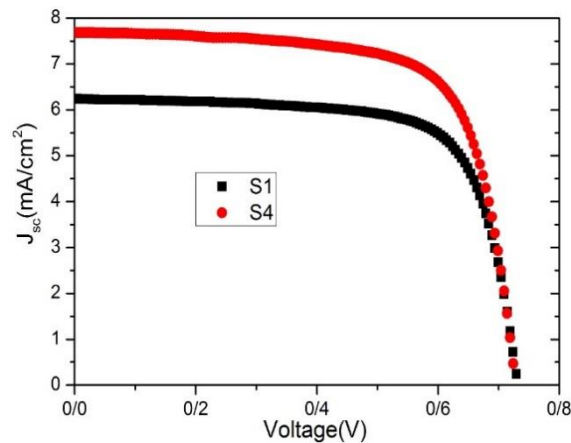


Fig.11. J-V plot of the cell fabricated using TiO<sub>2</sub> nanoparticles (S1) and nanorods (S4).

and 35 – 45 nm thickness. For S4 (Fig.9-S4) the colloidal solution is exposed by the excess of PVP and the morphology of nanostructures change dramatically to elongated nanorods. As the amount of PVP increased, the crystal facets of TiO<sub>2</sub> are more influenced by PVP adherence. It means that PVP would be attached to the lateral planes with high surface energy and doesn't allow the crystal to grow in that direction. It results to the formation of nanorods and nanowires. The more PVP is used, the better these facets are covered and thus longer and thinner they become (Fig.10).

The photocurrent density-voltage (J-V) and internal photocurrent efficiency (IPCE) characteristics of DSSC are depicted in Figs. 11 and 12, respectively. Samples with TiO<sub>2</sub> nanoparticles

and nanorods used as photoelectrode under simulated air mass 1.5 global (AM 1.5G) full sunlight intensity. Detailed photovoltaic parameters, namely, open-circuit voltage (V<sub>oc</sub>), short-circuit current density (J<sub>sc</sub>), fill factor (FF), and the photovoltaic power conversion efficiency (η) have been obtained and tabulated in Table 3. J<sub>sc</sub> is the parameter determined by the product of the charge carrier density under illumination, which shows the maximum number of the photo-generated carriers that can be extracted from a solar cell. The results demonstrated that the nominal values of J<sub>sc</sub> were lower than the case of nanoparticle. The nominal efficiency of the prepared cell with nanorods was also lower than the nanoparticle case. The results indicate low

Table 3. Cell performance parameters extracted from J-V plots of nanoparticles and nanorods used as photoanode.

Cell	V <sub>oc</sub> (v)	J <sub>sc</sub> (mA/cm <sup>2</sup> )	η(%)	FF (%)
S1	0.765	6.24	3.23	70.5
S4	0.765	7.5	4.01	72.1

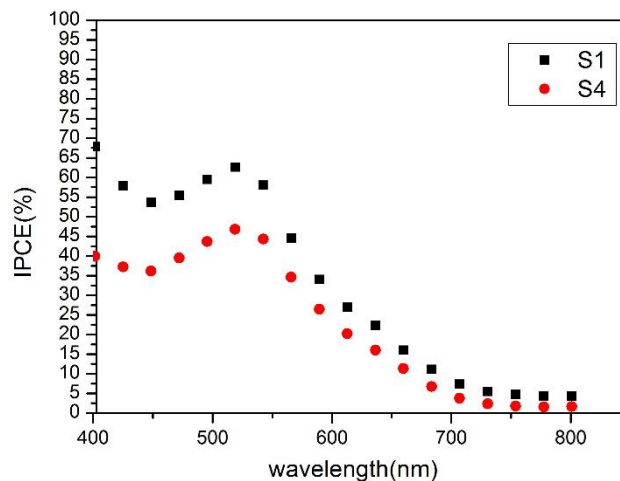


Fig.12. IPCE plot of the cell fabricated using TiO<sub>2</sub> nanoparticles (S1) and nanorods (S4).

photocurrent values compare to the reports for DSSCs [49-52]. IPCE values are indicating low values over visible to IR range which confirms low dye adsorption. This causes low performance of the solar cells. Although the IPCE of S4 is less than S1, the efficiency as well as J<sub>sc</sub> of S4 is higher than S1 nanoparticle samples. This may be due to better morphology and TiO<sub>2</sub>/organic interfacial interface and also could be the indication of the enhancement of electron transport rather than the particles which is confirmed also elsewhere [18]. It is also notable that high efficiency photoelectrode, in our research TiO<sub>2</sub> nanorods sample, for DSSCs requires not only a high surface area for the loading of large amounts of dye molecules but also a closed net microstructure for light capture and facile electron transport [53].

### CONCLUSIONS

Various TiO<sub>2</sub> nanostructures were fabricated using a microwave assisted solvothermal method. PVP and ascorbic acid (AA) were used as a surfactant and reducing agents, respectively. The results show that PVP/AA mole ratio has a crucial effect on the morphology of final powder. XRD analysis showed that both Anatase and Rutile phases are available in the powders but with the increase of

PVP/AA ratio, Anatase phase is only formed. Dye sensitized solar cell fabricated using TiO<sub>2</sub> nanorods showed an efficiency enhancement due to the enhancement of short current circuit. It indicated that nanorods enhanced electron transport due to their preferential growth morphology.

### ACKNOWLEDGMENT

This research was supported by Imam Reza International University of Mashhad under Grant No: 21703.

### CONFLICT OF INTEREST

The authors declare that there is no conflict of interests regarding the publication of this manuscript.

### REFERENCES

- Owen Byrne, Iftikhar Ahmad, Praveen K. Surolia, Yurii K.Gun'ko. The optimisation of dye sensitised solar cell working electrodes for graphene and SWCNTs containing quasi-solid state electrolytes. *Solar energy*. 2014, 10:239-246.
- Barbora Laskova, Marketa Zukalova, Arnost Zukal, Milan Bousa. Capacitive contribution to Li-storage in TiO<sub>2</sub> (B) and TiO<sub>2</sub> (anatase). *Journal of Power Sources*. 2014, 246:103-109.
- Liming Wu, Daniel Buchholz, Dominic Bresser, Luciana Gomes Chagas. Anatase TiO<sub>2</sub> nanoparticles for high



- power sodium-ion anodes. *Journal of Power Sources*. 2014, 251:379-385.
4. Mohammad Khaja Nazeeruddin, Etienne Baranoff, Michael Grätzel. Dye-sensitized solar cells: A brief overview. *Solar Energy*. 2011, 85:1172-1178.
  5. Zhen-Long Zhang, Jun-Feng Li, Xiao-Li Wang, Jian-Qiang Qin. Enhancement of Perovskite Solar Cells Efficiency using N-Doped TiO<sub>2</sub> Nanorod Arrays as Electron Transfer Layer. *Nanoscale Research Letters*. 2017, 12:43-50.
  6. Po-Shen Shen, Chuan-Ming Tseng, Ta-Chuan Kuo, Ching-Kuei Shih. Microwave-assisted synthesis of titanium dioxide nanocrystalline for efficient dye-sensitized and perovskite solar cells. *Solar Energy*. 2015, 120:345-356.
  7. Zainal Arifin, Suyitno Suyitno, Syamsul Hadi, Bayu Sutanto. Improved performance of dye-sensitized solar cells with TiO<sub>2</sub> nanoparticles/Zn-doped TiO<sub>2</sub> hollow fiber photoanodes. *Energies*. 2018, 11:2922-2933.
  8. Jung Eun Nam, Hyo Jeong Jo, Jin-Kyu Kang, Sungho Woo. Optimization of Electrolyte Components on the Performance of Organic-Dye-Sensitized Solar Cells. *Journal of Nanoscience and Nanotechnology*. 2017, 17:8100-8104.
  9. Jeong-Hwa Kim, Kun-Ho Jang, Shi-Joon Sung, Dae-Kue Hwang. Enhanced Performance of Dye-Sensitized Solar Cells Based on Electrospun TiO<sub>2</sub> Electrode. *Journal of Nanoscience and Nanotechnology*. 2017, 17:8117-8121.
  10. Yong-Min Lee, Dong In Kim, Ki-Hwan Hwang, Sang Hun Nam. Enhanced power conversion efficiency of dye-sensitized solar cells assisted with phosphor materials. *Electronic Materials Letters*. 2016, 12:512-516.
  11. Mojtaba Abdi-Jalebi, Aravind Kumar Chandiran, Mohammad Khaja Nazeeruddin, Michael Grätzel. Low temperature dye-sensitized solar cells based on conformal thin zinc oxide overlayer on mesoporous insulating template by atomic layer deposition. *Scientia Iranica F*. 2014, 21:2479-2484.
  12. Guihua Yu, Jing Gao, J. C. Hummelen, Fred Wudl. Polymer Photovoltaic Cells: Enhanced Efficiencies via a Network of Internal Donor-Acceptor Heterojunctions. *Science*. 1995, 270:1789-1791.
  13. T. V. Arjunan, T. S. Senthil. Dye sensitised solar cells. *Materials Technology*. 2013, 28:9-14.
  14. T. M. Razykov, N. Amin, M. Alghoul, B. Ergashev. Revolutionary novel and low cost CMBD method for fabrication of CdTe absorber layer for use in thin film solar cells. *Materials Technology*. 2013, 28:15-20.
  15. Ya Cao, Zhen Li, Yang Wang, Tao Zhang. Influence of TiO<sub>2</sub> Nanorod Arrays on the Bilayered Photoanode for Dye-Sensitized Solar Cells. *Journal of Electronic Materials*. 2016, 45:4989-4998.
  16. Oliver Ilerperuma. Gel polymer electrolytes for dye sensitised solar cells: a review. *Materials Technology*. 2013, 28:65-70.
  17. K. R. Justin Thomas, Abhishek Baheti. Fluorene based organic dyes for dye sensitised solar cells: structure-property relationships. *Materials Technology*. 2013, 28:71-87.
  18. Andrew Blakers, Ngwe Zin, Keith R. McIntosh, Kean Fong. High Efficiency Silicon Solar Cells. *Energy Procedia*. 2013, 33:1-10.
  19. Jae-Yup Kim, Jiwoong Yang, Jung Ho Yu, Woonhyuk Baek. Highly Efficient Copper-Indium-Selenide Quantum Dot Solar Cells: Suppression of Carrier Recombination by Controlled ZnS Overlayers. *ACS Nano*. 2015, 9:11286-11295.
  20. Hao Hu, Ka Kan Wong, Tom Kollek, Fabian Hanusch. Highly Efficient Reproducible Perovskite Solar Cells Prepared by Low-Temperature Processing. *Molecules*. 2016, 21:542-552.
  21. PilHo Huh, Seong-Cheol Kim. Easy formation and dye-sensitized solar cell application of highly-ordered 3D titania arrays using photodynamic polymer. *Electronic Materials Letters*. 2012, 8:131-134.
  22. Daniela Nunes, Ana Pimentel, Joana Vaz Pinto, Tomás Calmeiro. Photocatalytic behavior of TiO<sub>2</sub> films synthesized by microwave irradiation. *Catalysis Today*. 2016, 278:262-270.
  23. A. Mishra, Alok Kumar, D. Hodges, R. D. K. Misra. Tunable TiO<sub>2</sub>-pepsin thin film as a low-temperature electron transport layer for photoelectrochemical cells. *Journal Materials Technology*. 2017, 32:829-837.
  24. Peter Chen, Jérémie Brillet, Hari Bala, Peng Wang. Solid-state dye-sensitized solar cells using TiO<sub>2</sub> nanotube arrays on FTO glass. *Journal of Materials Chemistry*. 2009, 19:5325-5328.
  25. Daibin Kuang, Jérémie Brillet, Peter Chen, Masakazu Takata. Application of Highly Ordered TiO<sub>2</sub> Nanotube Arrays in Flexible Dye-Sensitized Solar Cells. *ACS Nano*. 2008, 2:1113-1116.
  26. P.A. van Hal, M. M. Wienk, J. M. Kroon, W. J. H. Verhees. Photoinduced Electron Transfer and Photovoltaic Response of a MDMO-PPV:TiO<sub>2</sub> Bulk-Heterojunction. *Advanced Materials*. 2003, 15:118-121.
  27. Lenneke Slooff-Hoek, M. M. Wienk, J. M. Kroon. Hybrid TiO<sub>2</sub>/polymer photovoltaic cells made from a titanium oxide precursor. *Thin Solid Films*. 2004, 451:634-638.
  29. Sayaka Yanagida, G. K. R. Senadeera, K. Nakamura, T. Kitamura. Polythiophene-sensitized TiO<sub>2</sub> solar cells. *Journal of Photochemistry and Photobiology A: Chemistry*. 2004, 166:75-80.
  30. Yongfang Jia, Feng Yang, Fanggong Cai, C. H. Cheng. Photoelectrochemical and Charge Transfer Properties of SnS/TiO<sub>2</sub> Hetero structure Nanotube Arrays. *Electronic Materials Letters*. 2013, 9:287-291.
  31. Chengkun Xu, Paul H Shin, Liangliang Cao, Jiamin Wu. Ordered TiO<sub>2</sub> Nanotube Arrays on Transparent Conductive Oxide for Dye-Sensitized Solar Cells. *Chemistry of Materials*. 2010, 22:143-148.
  32. Thomas Stergiopoulos, Anna Valota, Vlassis Likodimos, Thanassis Speliotis. Dye-sensitization of self-assembled titania nanotubes prepared by galvanostatic anodization of Ti sputtered on conductive glass. *Nanotechnology*. 2009, 20:365601.
  33. Tae-Sik Kang, Adam P Smith, Barney E Taylor, Michael F Durstock. Fabrication of Highly-Ordered TiO<sub>2</sub> Nanotube Arrays and Their Use in Dye-Sensitized Solar Cells. *Nano Lett*. 2009, 9:601-606.
  34. George Kenanakis, Dimitra Vernardou, A. Dalamagkas, N. Katsarakis. Photocatalytic electrooxidation properties of TiO<sub>2</sub> thin films deposited by sol-gel. *Catalysis Today*. 2015, 240:146-152.
  35. Hadj Benhebal, Messaoud Chaib, Angélique Léonard, Ludvine Tasseroul. Sol-gel preparation and characterisation of SnO<sub>2</sub> powders employed as catalyst for phenol photodegradation. *Scientia Iranica C*. 2013, 20:1891-1898.
  36. Ana Pimentel, Joana Rodrigues, Paulo Duarte, Daniela Nunes. Effect of solvents on ZnO nanostructures synthesized by solvothermal method assisted by microwave radiation: A photocatalytic study. *Journal of Materials*

- Science. 2015, 50:5777-5787.
37. Xiaobo Chen, Yuan Mao. Titanium Dioxide Nanomaterials: Synthesis, Properties, Modifications, and Applications. Chemical Reviews. 2007, 107:2891-2959.
  38. Hsin-Hung Ou, Shang-Lien Lo. Review of Titania Nanotubes Synthesized via the Hydrothermal Treatment: Fabrication, Modification, and Application. Separation and Purification Technology. 2007, 58:179-191.
  39. S. Das, Anoop Mukhopadhyay, Someswar Datta, D. Basu. Prospects of Microwave Processing: An Overview. Bulletin of Materials Science. 2009, 32:1-13.
  40. Kislá Siqueira, Roberto Luiz Moreira, Marcelo Valadares, Anderson Dias. Microwave-hydrothermal preparation of alkaline-earth-metal tungstates. Journal of Materials Science. 2010, 45:6083-6093.
  41. J. C. Sczancoski, L. S. Cavalcante, Miryam Rincón-Joya, J. A. Varela. SrMoO<sub>4</sub> powders processed in microwave-hydrothermal: Synthesis, characterization and optical properties. Chemical Engineering Journal. 2008, 140:632-637.
  42. Tomoko Kasuga, Masayoshi Hiramatsu, Akihiko Hoson, Tohru Sekino. Formation of Titanium Oxide Nanotube. Langmuir. 1998, 14:3160-3163.
  43. Tomoko Kasuga, Masayoshi Hiramatsu, Akihiko Hoson, Tohru Sekino. Titania Nanotubes Prepared by Chemical Processing. Advanced Materials. 1999, 11:1307-1311.
  44. Ke Fan, Wei Zhang, Tianyou Peng, Junnian Chen. Application of TiO<sub>2</sub> Fusiform Nanorods for Dye-Sensitized Solar Cells with Significantly Improved Efficiency. The Journal of Physical Chemistry C. 2011, 115:17213-17219.
  45. G. K. Williamson, W. H. Hall. X-ray line broadening from filed aluminium and wolfram. *L'élargissement des raies de rayons x obtenues des limailles d'aluminium et de tungstène*. Die verbreiterung der roentgeninterferenzlinien von aluminium- und wolframspänen. Acta Metallurgica. 1953, 1:22-31.
  46. A. R. Stokes, A. J. C. Wilson. The diffraction of X rays by distorted crystal aggregates – I. Proceedings of the Physical Society. 1944, 56:174.
  47. Ali Khorsand Zak, Abd Majid W.H, Majid Ebrahimzadeh Abrishami, Ramin Yousefi. X-ray analysis of ZnO nanoparticles by Williamson–Hall and size–strain plot methods. Solid State Sciences. 2011, 13: 251-256.
  48. Arindam Ghosh, Navnita Kumari, S. Tewari, Ayon Bhattacharjee. Structural and optical properties of pure and Al doped ZnO nanocrystals. Indian Journal of Physics. 2013, 87:1099-1104.
  49. Masoud Karimpour, Sara Mashhoun, Mohsen Mollaei, Mehdi Molaei. A Simple Low Pressure Method for the Synthesis of TiO<sub>2</sub> Nanotubes and Nanofibers and Their Application in DSSCs. Electronic Materials Letters. 2015, 11:625-632.
  50. Emil Enache-Pommer, Janice E. Boercker, Eray Aydil. Electron transport and recombination in polycrystalline TiO<sub>2</sub> nanowire dye-sensitized solar cells. Applied Physics Letters. 2007, 91:123116 – 123118.
  51. Mahmoud Samadpour, A Irajizad, Nima Taghavinia, Morteza Molaei. A new structure to increase the photostability of CdTe quantum dot sensitized solar cells. Journal of Physics D Applied Physics. 2011, 44:045103-045109.
  52. Elham Ghadiri, Nima Taghavinia, Shaik M Zakeeruddin, Michael Graetzel. Enhanced Electron Collection Efficiency in Dye-Sensitized Solar Cells Based on Nanostructured TiO<sub>2</sub> Hollow Fibers. Nano Letters. 2010, 10:1632-1638.
  53. Hui Xu, Xia Tao, Dong-Ting Wang, Yan-Zhen Zheng. Enhanced efficiency in dye-sensitized solar cells based on TiO<sub>2</sub> nanocrystal/nanotube double-layered films. Electrochimica Acta. 2010, 55:2280-2285.